IEEE Robotics and Automation Letters (RA-L) paper, presented at ICRA 2026, Vienna, Austria. Cite as RA-L paper.

Distributed Multi-Robot Active-Sensing of a Diffusive Source

F. Pagano[1], N. De Carli[2], E. Restrepo[3], A. Marino[3], P. Robuffo Giordano[3]

***Abstract*—This paper considers the problem of coordinating a group of mobile robots for distributedly estimating the parameters of a diffusion model that generates a time-varying spatial field. We assume that each robot can measure the local concentration of a substance continuously released in the environment and base the proposed distributed estimation strategy on an Extended Information Consensus Filter (E-ICF) with a forgetting factor. We then develop a decentralized online motion strategy aimed at minimizing a Gramian-based information metric that improves the E-ICF convergence. Additional constraints, among which collision avoidance, are integrated as Control Barrier Functions (CBFs) in a Quadratic Program (QP). Finally, we present statistical comparisons against three baselines which show the improved performance of the proposed method in a range of simulated scenarios, and we also report the results of experiments carried out with quadcopters to demonstrate the actual implementability of the approach and its effectiveness in generating online, collision-free, and informative motions.**

***Index Terms*—Multi-Robot Systems, Distributed Robot Systems, Active-Sensing, Gramian**

I. Introduction

MOBILE multi-robot systems can be deployed as sensor networks to monitor environmental fields and physical quantities—such as temperature, chemical concentration, gas distribution, or radiation intensity. These systems can cooperatively estimate a quantity of interest while actively moving to maximize the collected information and, thus, improving the estimation performance (convergence rate and accuracy). Such methods, referred to as *active-sensing*, often rely on information-theoretic metrics derived from the Fisher Information Matrix (FIM) [1], the Gramian [2], [3], or the covariance matrix [4] for optimizing the robot motion.

In this paper, we propose a novel online, distributed, active sensing approach to estimate the parameters of a diffusive source in space with a team of mobile robots. Differently from previous works, we specifically address the case of a *continuously releasing source* whose model parameters are estimated with an Extended Information Consensus Filter (E-ICF). The active sensing strategy leverages the trace of the inverse of the Observability Gramian (OG) as information metric, and implements a decentralized gradient-based control algorithm for optimizing the robots' motions. To account for the lack of informative measurements when the robots are initially deployed far from the source, a mixed strategy is proposed to balance exploitation and exploration, using a convex combination of the OG-based input and a random one. Finally, a single optimization-based controller enforces constraints through Control Barrier Functions (CBFs) on the nominal input to ensure estimation convergence and safety.

A. Related Works

The problem of field reconstruction has been addressed in the literature with techniques such as Gaussian Process Regression (GPR) [5], [6], Variational Inverse Method [7], particle filter [8], radial basis functions and Kalman Filter [4]. Some applications focus solely on localizing the sources of a scalar field, which may be related to light [1], [9] or contaminants and odors [10]. In this context, source identification approaches aim at estimating the source properties by analyzing the signals it generates, whereas source seeking ones focus only on guiding the robots toward a field extremum, and thus to the source itself. If no prior knowledge on the source is assumed, the robots can estimate the gradient of the scalar field at the center of a symmetric formation [9], [11]–[14], and move along the gradient direction, or use it to bias a correlated random walk to balance exploitation and exploration [14]. Differently, in [15] the robotic swarm moves along the field ascending direction, lifting the formation constraint but assuming a bounded field gradient. Other approaches employ a measurement model with a Kalman Filter and then move the agents by leveraging the FIM [1] or the notion of confidence upper bound [16].

When the physics of the process can be assumed reasonably known, the estimation scheme can leverage physical models that are particularly useful for identifying a *diffusive* source. For instance, single-robot solutions include a PDE-constrained optimization to maximize the smallest eigenvalue of the FIM [17], and a model-based method to estimate the advection-diffusion parameters for an instantaneous gas release [18]. In the multi-robot setting, [19] combines constrained cooperative Kalman filtering, recursive least squares, and a finite-volume PDE approximation.

Persistent environmental monitoring for instantaneous gas releases is also addressed with a single robot [2] and with multiple robots [3] using the constructability Gramian—via a gradient-based control law in the former and a reinforcement learning-based distributed policy in the latter. In both methods, the task execution is encoded through constraints, while CBFs are used to include energy limits and achieve task persistency.

Manuscript received: April, 14, 2025; Revised June, 16, 2025; Accepted August, 18, 2025. This paper was recommended for publication by Editor M. Ani Hsieh upon evaluation of the Associate Editor and Reviewers' comments.

This work was supported by the COWBOT project in the frame of the PRIN 2020 research program, grant number 2020NH7EAZ 002, and by the ANR-20-CHIA-0017 project "MULTISHARED".

[1]F. Pagano is with Centro Servizi Metrologici e Tecnologici Avanzati (CeSMA), Corso Nicolangelo Protopisani, 80146, Naples, Italy francesca.pagano@unina.it.

[2]N. de Carli is with the Division of Decision and Control Systems, KTH Royal Institute of Technology, Stockholm, Sweden ndc@kth.se.

[3]E. Restrepo, A. Marino and P. Robuffo Giordano are with CNRS, Univ Rennes, Inria, IRISA – Rennes, France.{esteban.restrepo, antonio.marino, prg} @irisa.fr.

Digital Object Identifier (DOI): see top of this page.

IEEE Robotics and Automation Letters (RA-L) paper, presented at ICRA 2026, Vienna, Austria. Cite as RA-L paper.

B. Contributions

In this work, we propose an active sensing framework based on a closed-form solution of the diffusion equation, similarly to [2], [3], [18], where an instantaneous release model is introduced; however, contrary to these works, we consider here the case of a *continuously releasing source*. This modeling introduces additional challenges, as the field gradient can become unbounded, but it also more accurately captures diffusion processes, such as gas leaks, where the assumption of *instantaneous release* is quite unrealistic. For instance, in scenarios where a substance is continuously emitted, its concentration increases over time rather than decaying, making the proposed modeling a better choice for practical applications in environmental monitoring and hazard detection.

To the best of the authors' knowledge, no previous source estimation strategies have considered the continuous release model. Unlike [3], the proposed active sensing strategy does not require reinforcement learning but uses a simple, yet effective, gradient-based input, as done in [1], whose cost function shares a strong connection with the Gramian-based metric used in this work. However, [1] is exclusively focused on source seeking, whereas the proposed method does not necessarily require the robots to reach the source. Instead, the robot movement is driven by the objective of estimating the diffusion model parameters, which also include the source location. Nevertheless, because approaching the source location tends to increase information gain, the resulting active sensing strategy leads the robots closer to the source as a byproduct, rather than as an explicit goal. However, instead of following a direct path, the robots move to maximize information gain, exploring the environment in a way that enhances the estimation of the diffusion model parameters.

Our main contributions can be summarized as follows:

- A novel distributed active-sensing approach that leverages an **A**-optimality [20] Gramian-based information metric and a random strategy to estimate the parameters of a time-varying diffusive field.
- An extensive simulation campaign and a statistical analysis show that the proposed motion strategy improves estimation convergence, with more efficient motions compared to three baselines, particularly when robots are few.
- An experimental validation with multiple quadrotors and a simulated field shows the implementability of the proposed approach, generating online, collision-free, and informative motions in a decentralized manner.

The remainder of the paper is structured as follows. Section II introduces the problem modeling, Sec. III presents the proposed methodology, Sec. IV reports simulative results, and Sec. V experimental ones. The conclusions are in Sec. VI.

II. Problem Modeling

A. Robot model

Let us consider a team of N robots able to localize themselves in a common frame. Each agent communicates with its neighbors according to a fixed, undirected, and connected communication graph $\mathcal{G} = (\mathcal{V}, \mathcal{E})$, where $\mathcal{V}$ is the node set and $\mathcal{E} \subseteq \mathcal{V} \times \mathcal{V}$ is the edge set. The set of neighbors is indicated as $\mathcal{N}_i \triangleq \{j \in \mathcal{V} : (i,j) \in \mathcal{E}\}$. Each i-th robot is modeled as a single integrator

$$\dot{\mathbf{p}}_i = \mathbf{u}_i \quad \forall i = 1, ..., N \tag{1}$$

where $\mathbf{p}_i \in \mathbb{R}^3$ is the position vector and $\mathbf{u}_i \in \mathbb{R}^3$ the velocity input. The collective robot state is denoted with $\mathbf{p} = \left[\mathbf{p}_1^T, \mathbf{p}_2^T, \dots, \mathbf{p}_N^T\right]^T \in \mathbb{R}^{3N}$ containing the robot stacked positions.

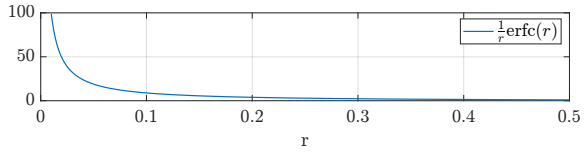

Fig. 1: Plot of ξ as a function of the Euclidean distance from the source, with $\phi/(4\pi D) = 1$, and $2\sqrt{Dt} = 1$.

B. Source model

We assume that each agent can measure the local concentration ξ of the released substance at its current position. To model this concentration, we employ a closed-form solution of the diffusion equation. Specifically, in an infinite isotropic medium[1] with a constant diffusion coefficient D, the diffusion equation for a continuous point source releasing a substance at a constant rate ϕ admits a closed-form solution. The corresponding concentration ξ at a point $\mathbf{q} \in \mathbb{R}^3$ and time t is given by [21]

$$\begin{aligned}\xi(\mathbf{q}, t) &= \frac{\phi}{4\pi D r} \operatorname{erfc}\left(\frac{r}{2\sqrt{Dt}}\right) \\ &= \frac{\phi}{4\pi D r}\left[1 - \frac{2}{\sqrt{\pi}} \int_0^{\frac{r}{2\sqrt{Dt}}} \exp\left(-\eta^2\right) d\eta\right],\end{aligned} \tag{2}$$

where $r = \|\mathbf{q} - \boldsymbol{\mu}\|$, with $\boldsymbol{\mu} \in \mathbb{R}^3$ being the source center location, and $\operatorname{erfc}(\cdot)$ is the *complementary error function*. The diffusion equation (2) can be leveraged for estimating both the source location $\boldsymbol{\mu}$ and the release rate ϕ, which in this work are treated as unknown constant parameters. This nonlinear estimation problem can be cast as a state-estimation problem using the measurement model as output function. Introducing the state variable $\mathbf{x} = \left[\boldsymbol{\mu}^T, \phi\right]^T \in \mathbb{R}^4$, the system model is

$$\begin{cases} \dot{\mathbf{x}} &= \mathbf{0} \\ y &= m(\mathbf{x}, \mathbf{q}, t) = \frac{\phi}{4\pi D \|\mathbf{q}-\boldsymbol{\mu}\|} \operatorname{erfc}\left(\frac{\|\mathbf{q}-\boldsymbol{\mu}\|}{2\sqrt{D(t+\tau_0)}}\right), \end{cases} \tag{3}$$

where $\tau_0 \in \mathbb{R}^+$ is used to account for the instant at which the diffusion starts. The value of τ_0 is here assumed known, but future work could include this parameter too in the estimation.

The concentration measure increases monotonically as the distance from the source location decreases, as depicted in Fig. 1. Moreover, both the concentration and the gradient of the measurement function (3) diminish as they move away from the source and grow unbounded towards the center; this poses some challenges to the estimation, as will be discussed in the following.

[1]We highlight that the isotropic model also applies to some anisotropic problems that can be transformed into equivalent isotropic ones [21, Sec.1.4].

IEEE Robotics and Automation Letters (RA-L) paper, presented at ICRA 2026, Vienna, Austria. Cite as RA-L paper.

III. METHODOLOGY

This section describes the proposed methodology. Sec. III-A presents the E-ICF, Sec. III-B introduces the Gramian-based information measure, Secs. III-Cand III-D describe the active-sensing strategy, and Sec. III-E the CBFs-based quadratic problem.

A. Information Consensus Filter

The robots run an extended ICF to iteratively estimate the parameters $\mathbf{x}$ in a distributed way. This filter, originally presented in [22] in a linear setting, is particularly useful in the presence of naive sensors, i.e., sensors that are neither sensing directly nor are neighbors to a sensing node. This aspect is particularly relevant as the measurement function (2) quickly decreases to zero far from the source, meaning that robots are likely to become uninformed.

In this work, a nonlinear version of the filter, similar to the one proposed in [23], is applied with the addition of a forgetting factor. The Extended-ICF algorithm employed is briefly described in the following. At time t_k, the $i-$th robot samples a measure y_i and updates the local information matrix $\mathbf{W}_i^0$ and information vector $\mathbf{w}_i^0$ using the prior information matrix $\mathbf{\Omega}_i^-$ and the local measurement only, as

$$\mathbf{W}_i^0 = \mathbf{\Omega}_i^- + \mathbf{C}_i^T \lambda_i \mathbf{C}_i, \tag{4}$$

$$\mathbf{w}_i^0 = \mathbf{\Omega}_i^- \hat{\mathbf{x}}_i^- + \mathbf{C}_i^T \lambda_i z_i, \tag{5}$$

where $z_i = y_i - m_i(\hat{\mathbf{x}}_i^-, \mathbf{p}_i, t_k) + \mathbf{C}_i(\hat{\mathbf{x}}_i^-, \mathbf{p}_i, t_k)\hat{\mathbf{x}}_i^-$ is the virtual measurement [23], $\mathbf{C}_i$ is the output matrix of the linearized system, and λ_i is the inverse of the output noise covariance w. Then, L rounds of average consensus iterations are performed, obtaining $\mathbf{W}_i^L$ and $\mathbf{w}_i^L$. Finally, the posteriors are updated as $\hat{\mathbf{x}}_i^+ = (\mathbf{W}_i^L)^{-1}\mathbf{w}_i^L$, and $\mathbf{\Omega}_i^+ = \mathbf{W}_i^L$. The new prior covariance $\mathbf{\Omega}_i^-$ is obtained with the addition of a forgetting factor [24] specified by a diagonal positive definite matrix $\mathbf{\Gamma}$, as $\mathbf{\Omega}_i^- = (\mathbf{I} - \mathbf{\Gamma})\left(\mathbf{Q} + \mathbf{\Omega}_i^+\right)^{-1} + \mathbf{\Gamma}\bar{\mathbf{\Omega}}$, where $\bar{\mathbf{\Omega}}$ is a minimum bound on the information that can be chosen as the inverse of the maximum estimation covariance, and $\mathbf{Q}$ is a positive definite matrix. The inclusion of a forgetting factor helps prevent estimator overconfidence, enhances filter stability, and can improve the convergence rate [25, Chap.6]. Finally, the prediction step is performed enforcing bounds on the state.

B. Information metric

The local Observability Gramian was introduced in [26] as a quantifiable measure of observability for nonlinear systems. In particular, if the OG is full rank over a time interval, the system is locally weakly observable [27]. The Gramian is computed by linearizing the system around a nominal trajectory [28] and has been widely used in active sensing applications to both quantify and optimize observability, ultimately guiding the design of informative trajectories. Formally, the Observability Gramian $\mathbf{G}(t_0, t_f) \in \mathbb{R}^{n\times n}$ is defined as[2]

$$\mathbf{G}(t_0, t_f) \triangleq \int_{t_0}^{t_f} \mathbf{\Phi}(\tau, t_0)^T \mathbf{C}^T(\tau)\mathbf{C}(\tau)\mathbf{\Phi}(\tau, t_0) d\tau \tag{6}$$

[2]The integral of a matrix is here intended as the integral of the single components.

with $t_f > t_0$, and where $\mathbf{\Phi}(\tau, t_0) \in \mathbb{R}^{n\times n}$ is the state transition matrix of the linearized system to be observed [28], having indicated with n the state dimension.

In this work, we consider multiple robots cooperatively estimating the source parameters, and thus, we necessitate a collective measure of information. The *collective* OG, which represents the information acquired by all robots up to time t, is expressed, similarly to [29], as:

$$\mathbf{G}(t) = \mathbf{G}(t_0) + \int_{t_0}^{t} \sum_{i=1}^{N} \mathbf{C}_i(\tau)^T \mathbf{C}_i(\tau)\, d\tau, \tag{7}$$

where $\mathbf{G}(t_0) = \mathbf{G}_0 \in \mathbb{R}^{4\times 4}$ represents the initial information at time t_0, and the second term captures the cumulative contributions of all robots. Furthermore, we note that for model (1) $\mathbf{\Phi}(\tau, t_0) = \mathbf{I}$, for all τ, and that matrix $\mathbf{C}_i^T\mathbf{C}_i$ is positive semi-definite and, therefore, the information monotonically increases in time. To prevent unbounded growth of information, the expression above can be modified to include a forgetting factor, which causes the Gramian matrix entries to decay exponentially in the absence of new information [29]. By including this modification, the Gramian dynamics becomes:

$$\dot{\mathbf{G}}(t) = -k\left(\mathbf{G}(t) - \bar{\mathbf{G}}\right) + \underbrace{\sum_{i=1}^{N} \mathbf{C}_i(\mathbf{p}_i, t)^T b_i \mathbf{C}_i(\mathbf{p}_i, t)}_{\mathbf{X}(t,\mathbf{p})}, \tag{8}$$

where k is a positive constant scalar forgetting factor, $\bar{\mathbf{G}}$ is a symmetric positive definite matrix that represents a lower bound on the minimum information [24], $\mathbf{X}(t, \mathbf{p})$ represents the new information matrix acquired through the current estimation and b_i is a positive scalar weighting the information being acquired by the i-th robot.

Remark 1: *The forgetting term in* (8) *ensures that the Gramian remains both upper- and lower-bounded, preventing numerical issues. Additionally, it gradually discards outdated information, encouraging information acquisition over time.*

Since the concentration ξ grows unbounded near the source location, and so does its gradient $\mathbf{C}_i$, to guarantee a bounded information term the robots must not approach too closely the estimated source position $\hat{\boldsymbol{\mu}}$. This is achieved by imposing a minimum distance $r_{min} > 0$ of each robot from $\hat{\boldsymbol{\mu}}$ as

$$\|\mathbf{p}_i - \hat{\boldsymbol{\mu}}\| > r_{min} \implies \exists\, \delta(r_{min}) : \mathbf{C}_i^T b_i \mathbf{C}_i < \delta(r_{min})\mathbf{I}. \tag{9}$$

This constraint is enforced through a suitable barrier function as discussed in Sec. III-E.

In the following, leveraging the OG as information matrix, we adopt the $\mathbf{A}$-optimality criterion [20, Sect.6.3], defined as:

$$V \triangleq \operatorname{tr}\left(\mathbf{G}(t)^{-1}\right), \tag{10}$$

as information metric, where $\mathbf{G}$ is the Gramian matrix in (8). Widely used in optimal experimental design, this criterion is directly linked to the average estimation uncertainty and is typically minimized to improve accuracy.

IEEE Robotics and Automation Letters (RA-L) paper, presented at ICRA 2026, Vienna, Austria. Cite as RA-L paper.

C. Active sensing

The full system state is defined by combining the robot dynamics (1) with the OG evolution (8) into a single state vector $\boldsymbol{\zeta} = \left[\mathrm{vec}\left(\mathbf{G}\right)^T,\ \mathbf{p}^T\right]^T \in \mathbb{R}^{16+3N}$, where $\mathrm{vec}(\cdot)$ indicates the vectorization operator. The system evolution is then given by the following second-order system

$$\dot{\boldsymbol{\zeta}} = \mathbf{f}(\boldsymbol{\zeta}, t) + \mathbf{g}\mathbf{u} \tag{11}$$

$$= \begin{bmatrix} \mathrm{vec}\left(-k\left(\mathbf{G} - \bar{\mathbf{G}}\right) + \mathbf{X}(t, \mathbf{p})\right) \\ \mathbf{0}_{3N} \end{bmatrix} + \begin{bmatrix} \mathbf{0}_{16\times 3N} \\ \mathbf{I}_{3N} \end{bmatrix} \mathbf{u}, \tag{12}$$

where the vector $\mathbf{u} = \left[\mathbf{u}_1^T, \ldots, \mathbf{u}_N^T\right]^T \in \mathbb{R}^{3N}$ is the stacked vector of the robots' control inputs. Consequently, the information metric (10) has relative degree $r = 2$ with respect to $\mathbf{u}$, meaning it can only be influenced by the control input through its second time derivative, and thus cannot be minimized directly. For brevity, we omit the complete expression of the second derivative $\ddot{V}$ and present only the term that explicitly depends on the input $\mathbf{u}$, which is

$$L_{\mathbf{g}}\dot{V}\mathbf{u} = -\sum_{i=1}^{N}\sum_{j=1}^{4}\left(2b_i\mathbf{G}^{-1}\mathbf{C}_i^T\mathbf{u}_i^T\mathbf{J}_i^T\mathbf{G}^{-1}\right)_{jj} \tag{13}$$

$$= -\sum_{i=1}^{N}\sum_{j,k=1}^{4}\sum_{r=1}^{3} 2b_i(\mathbf{G}^{-1})_{jk}(\mathbf{C}_i)_k\ (\mathbf{u}_i)_r\ (\mathbf{J}_i)_{kr}\ (\mathbf{G}^{-1})_{kj}$$

where $L_{\mathbf{g}}\dot{V}$ denotes the Lie derivative of $\dot{V}$ along the vector field $\mathbf{g}$, while $(\cdot)_{jk}$ indicates an element in the j-th row and the k-th column, and with $\mathbf{J}_i = \frac{\partial \mathbf{C}_i^T(\mathbf{p}_i, t)}{\partial \mathbf{p}_i} \in \mathbb{R}^{4\times 3}$. Thus, the $i-$th robot control input can be designed from (13) as:

$$\mathbf{u}_i^g :\ = -\bar{u}\frac{L_{\mathbf{g}_i}\dot{V}^T}{\|L_{\mathbf{g}_i}\dot{V}\|}, \tag{14}$$

$$\left(L_{\mathbf{g}_i}\dot{V}\right)_r = -\operatorname{tr}\left(2b_i\mathbf{G}^{-1}\mathbf{C}_i\ (\mathbf{J}_i)_{*r}\mathbf{G}^{-1}\right).$$

This input optimizes the robot velocity direction while keeping a desired (and tunable) constant speed $\bar{u} \in \mathbb{R}_{>0}$.

The velocity input (14) implements the active sensing strategy by steering the robots in a direction that reduces $\dot{V}$. While the goal is to reduce V over time, its nonlinear dependence on the system state and relative degree two make direct minimization difficult. Instead, the controller follows a greedy strategy that seeks to locally minimize $\dot{V}$, which reflects the most informative direction based on current knowledge. This does not ensure a pointwise decrease of V—especially when the forgetting term dominates—but it encourages information gathering. A similar derivation of the gradient-based input was done in [30] to maximize the minimum eigenvalue of the OG, albeit for a different active-sensing problem. Notice also that the derived expression requires knowledge of matrix $\mathbf{G}(t)$, which can be obtained by integrating (8). In fact, even though the term $\mathbf{X}(t, \mathbf{p})$ contains collective information, each agent can compute it via a consensus algorithm, thus only requiring communication with neighboring robots. To this end, the consensus iterations already performed in the filter can also be exploited to reach agreement on $\mathbf{X}$. In this way, if all OGs are initialized with the same initial value, they share the same dynamics up to the consensus error on $\mathbf{X}$. This choice enables each robot to execute the active sensing strategy using only local information, namely the current estimated parameters from the E-ICF and the Gramian matrix.

D. Explorative motions

As the substance concentration diminishes with distance, the robots' initial measurements may be largely uninformative and dominated by noise. Consequently, the robots may lack sufficient information to determine a direction based on the active sensing input in (14). To address this problem, we propose a mixed strategy that includes an exploratory phase during the estimation process. This phase enables the robots to search for more meaningful measurements before fully relying on the Gramian-based input (14). The proposed i-th robot nominal control input $\mathbf{u}_i^d$ is selected as a linear combination of the gradient-based control law in (14), here indicated with $\mathbf{u}_i^g$, and an explorative input $\mathbf{u}_i^r \in \mathbb{R}^3$, as:

$$\mathbf{u}_i^d = \sigma_i(t)\mathbf{u}_i^g + (1 - \sigma_i(t))\mathbf{u}_i^r. \tag{15}$$

The blending function $\sigma_i(t) \in \mathbb{R}$ is designed as

$$\sigma_i(t) = \exp\left(-\frac{1}{1 - z_i^2(\hat{\phi})} + 1\right), \tag{16}$$

$$\dot{z}_i(t) = \begin{cases} 0 & \text{if } (z_i = 0 \wedge (\phi_{min} - \hat{\phi}_i) < 0) \vee \\ & (z_i = 1 - \epsilon \wedge (\phi_{min} - \hat{\phi}_i) > 0) \\ k_z(\phi_{min} - \hat{\phi}_i) & \text{otherwise,} \end{cases}$$

with $k_z > 0$ being a scalar gain, ϕ_{min} a minimum value of the release rate, and $\epsilon > 0$ an arbitrary small constant to ensure the definiteness of Eq. (16). Here, $\sigma_i(t)$ allows for a smooth switch to the explorative input when the estimated release rate tends to zero due to the absence of measurements. As soon as nonzero measurements are available, $\hat{\phi}_i$ increases and σ_i converges to one, forcing the robot to move using only the Gramian-based velocity input. Note that this switching mechanism operates collectively as it leverages the release rate estimated by all robots through the E-ICF filter. However, for this strategy to be effective, the robot measurement must remain non-zero for a sufficient duration to allow the filter to update the current estimate. From now on, this control input is referred to as RG, while the one employing only the term $\mathbf{u}_i^g$ is named OG.

E. Quadratic program

To ensure additional constraints, the nominal velocity input $\mathbf{u}_i^d$ implementing the active sensing strategy can be modified in a minimally invasive fashion using CBFs [31] and by solving the following Quadratic Problem (QP):

$$\min_{\mathbf{u}_i, \delta} \|\mathbf{u}_i - \mathbf{u}_i^d\|^2 + l\delta^2 \tag{17}$$

$$\dot{h}_s(\mathbf{p}_i, \hat{\boldsymbol{\mu}}_i) \geq -\gamma_s(h_s) + \delta, \tag{18}$$

$$\dot{h}_a^j(\mathbf{p}_i, \mathbf{p}_j) \geq -\gamma_a(h_a^j) \quad \forall j \in \{1, \ldots N\},\ j \neq i, \tag{19}$$

$$\dot{h}_b^{r+}(\mathbf{p}_i) \geq -\gamma_b(h_b^{r+}),$$

$$\dot{h}_b^{r-}(\mathbf{p}_i) \geq -\gamma_b(h_b^{r-}),\ r \in \{x, y, z\} \tag{20}$$

$$\|\mathbf{u}_i\|_\infty \leq u_{max}, \tag{21}$$

IEEE Robotics and Automation Letters (RA-L) paper, presented at ICRA 2026, Vienna, Austria. Cite as RA-L paper.

where $\delta \in \mathbb{R}$ is a slack variable, $l > 0$, and γ_s, γ_a, γ_b extended class $\mathcal{K}$ functions for the control barrier functions detailed below. Eq. (18), with the CBF $h_s = \|\mathbf{p}_i - \hat{\boldsymbol{\mu}}_i\|^2 - r_{min}^2$, enforces the constraint (9) for keeping the robots at a minimum distance r_{min} from the estimated source located in $\hat{\boldsymbol{\mu}}_i$. Since the location of the new estimated source could violate the constraint, (18) should be relaxed with the slack variable δ. The inter-agents collision avoidance constraint is implemented in (19), where $h_a^j = \|\mathbf{p}_i - \mathbf{p}_j\|^2 - d_{min}^2$, $\mathbf{p}_j$ and $\mathbf{p}_j$ represent the position of the $j-$th and $i-$th robot, respectively, and d_{min} is a minimum distance between agents. In the time derivative of h_a^j in (19), the $j-$th robot is considered static because its velocity input is assumed unavailable to the $i-$th robot, due to the decentralized implementation.

Eq. (20) enforces boundary constraints on a convex volume; the CBFs are defined for each coordinate r as $h_b^{r+} = l_{max}^r - b_d - (\mathbf{p}_i)_r$, $h_b^{r-} = -l_{min}^r - b_d + (\mathbf{p}_i)_r$, where $-l_{min}^r$, l_{max}^r are the area's limits, and b_d is a minimum distance. Finally, (21) implements input limits. Since the robots are modeled as single integrators and constraint (18) is relaxed, assuming every robot executes the same controller, the QP is always feasible if the initial state satisfies all safety constraints (i.e., h_b^{r-}, h_b^{r+}, and $h_a^j > 0 \ \forall j$), as the zero input $\mathbf{u}_i = \mathbf{0}$ satisfies all CBFs.

IV. Simulation results

In this section, we present the results of numerical simulations for evaluating the proposed strategy in a set of randomized scenarios. The results of 100 simulations, lasting 200 s each, are analyzed for a group of $N = \{2, 3, 4\}$ robots with nominal velocity norm $\bar{u} = 1$ m/s.

The initial source estimate is chosen as $\mathbf{x}_0 = [0, 0, 1.5, 2]^T$ in all simulations, while the robots initial positions are randomly sampled in a torus centered at $\hat{\boldsymbol{\mu}}$ with inner and outer radii $r_i = 0.2$ m and $r_o = 2.0$ m, respectively; samples violating the area bounds or the inter-agent minimum distance are discarded. The source parameters are instead sampled from a normal distribution centered at the initial estimate with standard deviations $\sigma_{\mu_x} = \sigma_{\mu_y} = 4$, $= \sigma_{\mu_z} = 2$, $\sigma_\phi = 1$. The measure noise covariance is $w = 1e^{-5}$, while the forgetting factors are $k = 1$ and $\boldsymbol{\Gamma} = \mathrm{diag}\big([1e^{-3}, 1e^{-3}, 1e^{-3}, 1e^{-2}]\big)$. The success rate of the source estimation task is evaluated against three baseline strategies chosen to represent typical, more heuristic approaches to source estimation: moving towards the estimated source (S), moving randomly (R), and combining the previous two approaches (RS). The control inputs for the implemented strategies are summarized below:

- Source direction (S)

$$\mathbf{u}_i^d = \bar{u} \frac{(\hat{\boldsymbol{\mu}}_i - \mathbf{p}_i)}{\|\hat{\boldsymbol{\mu}}_i - \mathbf{p}_i\|}. \tag{22}$$

- Random direction (R),

$$\mathbf{u}_i^d = \bar{u} \frac{\mathbf{v}_i}{\|\mathbf{v}_i\|}, \quad \dot{\mathbf{v}}_i = k_a \boldsymbol{\alpha}_i^r. \tag{23}$$

- Random and Source direction (RS)

$$\mathbf{u}_i^d = \bar{u} \frac{\mathbf{v}_i}{\|\mathbf{v}_i\|}, \quad \dot{\mathbf{v}}_i = k_r \frac{\boldsymbol{\alpha}_i^r}{\|\boldsymbol{\alpha}_i^r\|} + k_s \frac{(\hat{\boldsymbol{\mu}}_i - \mathbf{p}_i)}{\|\hat{\boldsymbol{\mu}}_i - \mathbf{p}_i\|}. \tag{24}$$

TABLE I: Comparison results

Metric	Method			
$\#\Big(\|\mathbf{e}_\mu\| \leq 0.02$ and $\|e_\phi\| \leq 0.1\Big)$	S	R	RS	RG (Proposed)
$N = 2$	0	8	36	64
$N = 3$	60	19	70	91
$N = 4$	81	44	96	96

- Gramian-Random direction (RG) using the input in (15) with $\mathbf{u}_i^r$ as in (24).

The quantities k_a, k_r, and k_s are positive scalar weights, and $\boldsymbol{\alpha}_i^r$ is obtained by sampling each element of the acceleration vector from a normal distribution. The QP safety layer described in Sec. III-E is applied in all cases. We note that the baseline strategy S is purely exploitative and lacks any exploratory behavior, while strategy R is exclusively explorative. In contrast, the RS strategy merges both behaviors.

The evaluated metrics are the estimation errors $\|e_\phi\| = |\phi - \hat{\phi}|$ and $\|\mathbf{e}_\mu\| = \|\boldsymbol{\mu} - \hat{\boldsymbol{\mu}}\|$ at the end of each simulation, referred to the first agent, and the effort computed as $L_s = \int_0^{t_f} \|\mathbf{u}\| dt$, where t_f is the time at which the parameters are considered successfully identified. The identification is considered successful if the estimation errors are below a given threshold ($\|e_\phi\| < 0.1$ and $\|\mathbf{e}_\mu\| < 0.02\ m$). Table I summarizes the number of successful source identifications according to the chosen threshold, while Fig. 2 contains the boxplots obtained by varying the motion strategy and the number of robots. Note that the non-negligible number of outliers (indicated with a red cross) is primarily due to two factors. First, the simulation time was fixed (i.e., convergence might still have occurred given enough additional time). Second, the estimation unavoidably fails to converge when the robots cannot measure the field.

To identify statistically relevant differences, a nonparametric test is employed for pairwise comparisons, given that the samples do not satisfy the normality assumption. Specifically, the Wilcoxon rank-sum test is applied with a 5% significance level ($p = 0.05$). In the case $N = 2$, the approach RG reveals statistically relevant differences on both $\|e_\phi\|$ and $\|\mathbf{e}_\mu\|$ if compared to S and R, and only on the metric $\|e_\phi\|$ ($p = 2.97e^{-5}$) when compared to RS.

In the scenario $N = 3$, the null hypothesis is rejected on both error metrics for the pairs RG-S and RG-R; and on the metric $\|e_\phi\|$ (p-value 0.04) with the pair RG-RS. Finally, with $N = 4$, the null hypothesis is rejected on both error metrics for the pairs S-RG and R-RG, and only on the metric $\|e_\phi\|$ (p-value $6.98e^{-4}$) for the pair RS-RG. Plots in Fig. 2 show that these differences correspond to lower medians of the error metrics obtained by method RG when compared to all the baselines for $N = \{2, 3\}$. In the case $N = 4$, RG performs better than the strategies S and R, while RS achieves a smaller median on $\|e_\phi\|$; however, both median values are below the selected threshold. Indeed, Tab. I highlights that the proposed method achieves a higher or equal number of successes in all the analyzed scenarios, obtained varying N.

While the RS and RG approaches have relevant similarities, significant differences are visible when analyzing the metric L_s. The results reported in Fig. 3 show that the RG approach

IEEE Robotics and Automation Letters (RA-L) paper, presented at ICRA 2026, Vienna, Austria. Cite as RA-L paper.

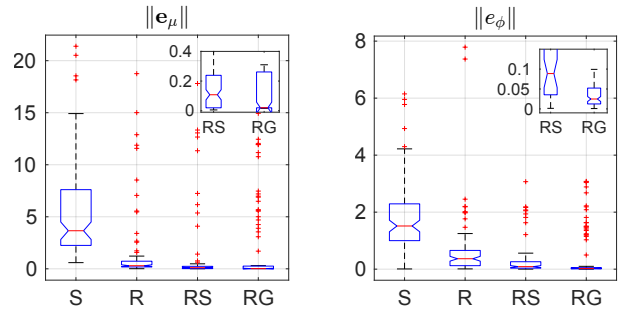

(a) $N = 2$

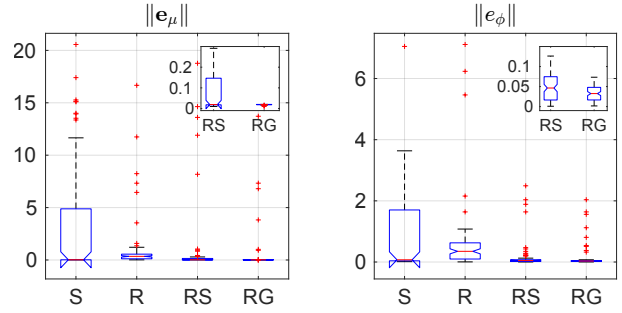

(b) $N = 3$

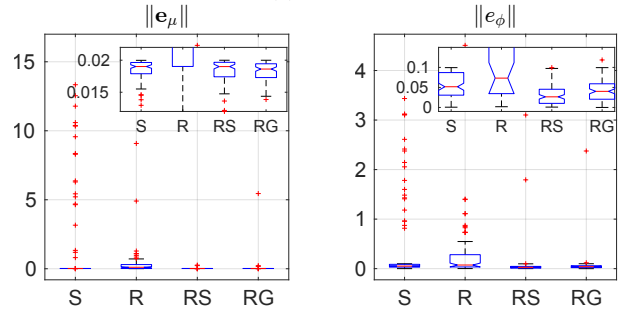

(c) $N = 4$

Fig. 2: Box plots comparing the estimation errors $\|e_\phi\|$, $\|\mathbf{e}_\mu\|$, varying the motion strategies {S, R, RS, RG} and the number of robots N. Boxes are in blue, with median values (red lines), confidence intervals (black lines), and outliers (red crosses). The upper right insets show zoomed-in views.

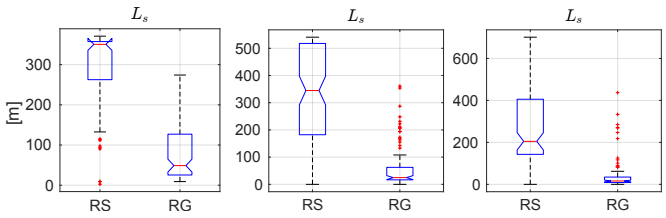

(a) $N = 2$ (b) $N = 3$ (c) $N = 4$

Fig. 3: Box plots comparing the metric L_s obtained with the motion strategies {RS, RG} and with N={2,3,4}.

generates more efficient motions when compared to the RS one, with better or comparable performance in terms of estimation error and success rate.

The reported results show that mixed strategies outperform the naive approach of moving towards the estimated source (S) in estimating the unknown parameters, thanks to both exploitative and explorative behaviors. However, the S approach improves significantly as the number of robots increases, as with more agents, less exploration is needed. In fact, in all cases, an increased number of robots improves the estimation success rate, as obviously expected. This is due to two main factors: using more agents increases the likelihood that at least one robot will measure the field; the estimation problem is better conditioned with $N = 4$, as the number of measurements equals the number of unknown parameters. Therefore, when employing a larger number of robots, optimizing the motion strategy becomes less critical for successful task execution; however, active sensing remains essential when only a few robots are available and the number of measures is less than the number of parameters to be estimated. Ultimately, in the analyzed scenarios, the proposed motion strategy can be beneficial in minimizing the number of required agents, the energy, and improving the estimation convergence.

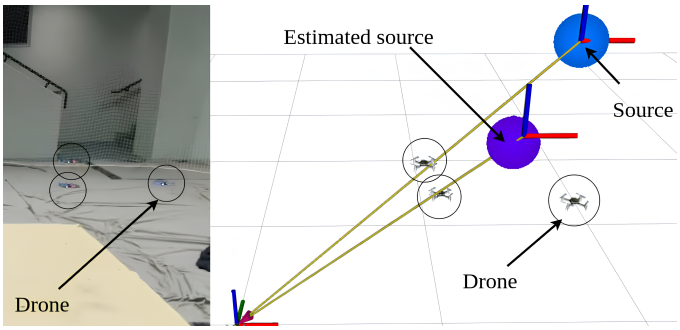

Fig. 4: Three crazyflies move to actively identify a simulated source.

V. Experimental Results

To validate the proposed methodology on real robotic systems, we conducted a series of experimental tests using Crazyflie[3] quadrotors in an indoor flight arena equipped with a motion capture system, as visible in Fig. 4. The code employed ROS2 and some of the functionalities provided by the Crazyswarm [32] framework. The source measurements were simulated using model (3) with an additive white noise with covariance $w = 1e^{-4}$. The forgetting factors were selected as $k = 0.05$ and $\mathbf{\Gamma} = 5\,\mathrm{diag}\big([1e^{-5}, 1e^{-5}, 1e^{-5}, 1e^{-4}]\big)$.

The results of three experimental tests with $N = 2$, $N = 3$, and $N = 4$ are reported in Figs. 5, 6, and 7, respectively, using the OG-based active-sensing strategy.

In detail, Fig. 5a shows the quadrotor paths retrieved with the motion capture system with continuous lines. The true source location is marked with a star, while the evolution of the estimated source, $\hat{\boldsymbol{\mu}}$, is also represented by a continuous line. The shaded sphere represents the distance from the source constraint encoded in (18), and is depicted only around the final estimation for visualization purposes. Fig. 5a shows the drones approaching the estimated source, as its estimate varies in time, and, once the estimation has converged, they start circling motions around the source. Figure 5b depicts the time

[3]https://www.bitcraze.io

IEEE Robotics and Automation Letters (RA-L) paper, presented at ICRA 2026, Vienna, Austria. Cite as RA-L paper.

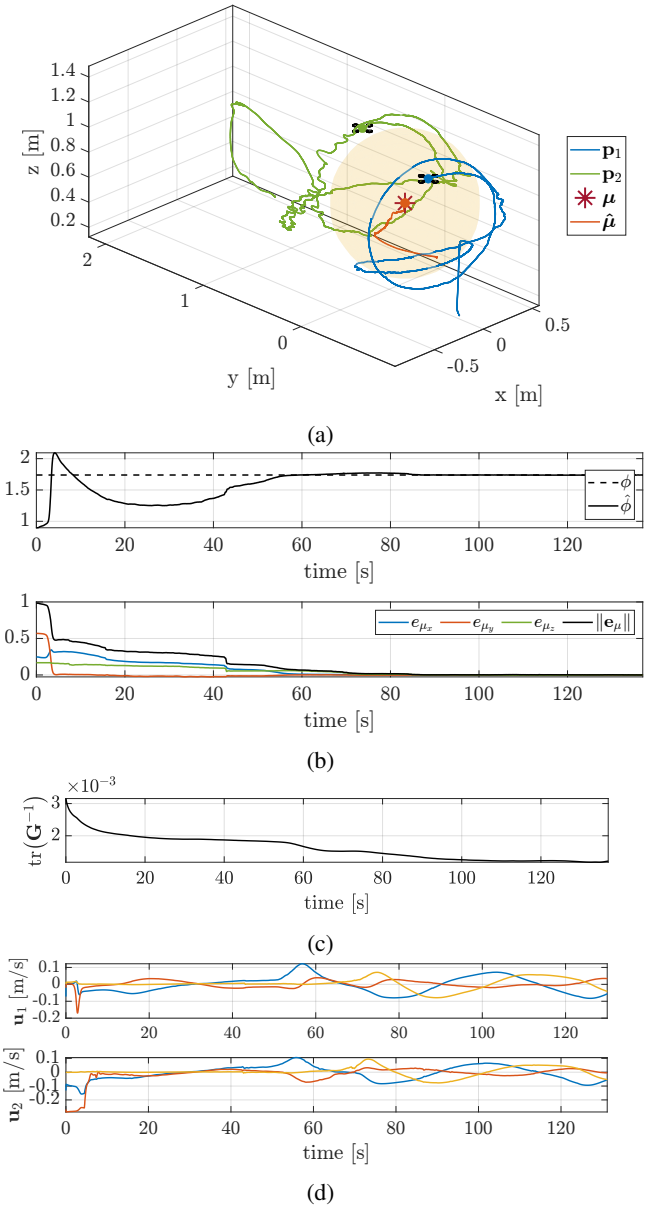

Fig. 5: $N = 2$, $\bar{u} = 0.3\ m/s$ (a) Drones' paths acquired from the motion capture system, the source location $\boldsymbol{\mu}$ is indicated with a star, and $\hat{\boldsymbol{\mu}}$ is the evolution of the location estimation. The depicted sphere is centered at the final estimated source and has radius r_{min}. (b) Evolution of $\hat{\phi}$ (top), source estimation error (bottom). (c) Evolution of V. (d) Inputs $\mathbf{u}_1$ and $\mathbf{u}_2$.

evolution of the estimated release rate $\hat{\phi}$ and its true value (top); and the error $\mathbf{e}_\mu$ (bottom). Fig. 5c shows the evolution of the information metric, expressed in (10). Both quantities are referred to the first agent, as no appreciable differences could be observed among agents, thanks to the consensus rounds. Finally, Fig. 5d contains the velocity inputs computed after the QP . Notice that, despite enforcing a constant nominal velocity $\bar{u} = 0.3$ m/s, the actual agents' velocities were modified by the QP layer, resulting in slower motions.

Analogously, the results of the second and third experiments are presented in Fig. 6 and 7. In all cases, the estimation

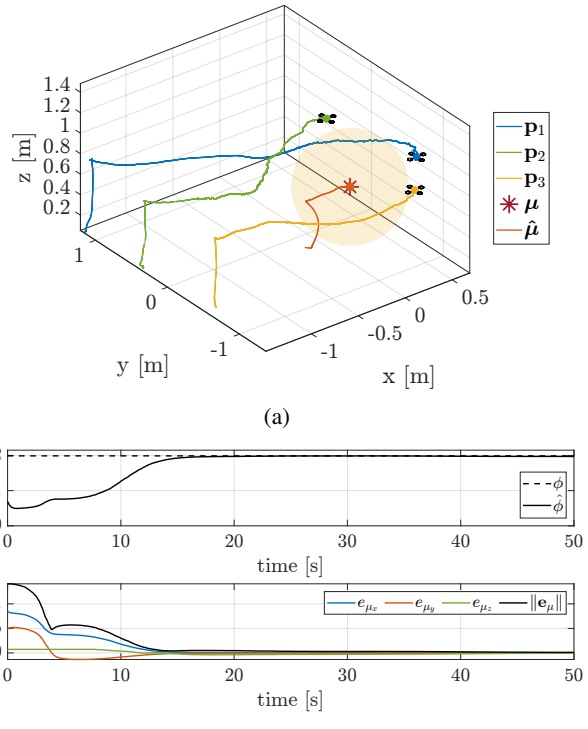

Fig. 6: $N = 3$, $\bar{u} = 0.2\ m/s$ (a) Drones' paths acquired from the motion capture system, the source location $\boldsymbol{\mu}$ is indicated with a star, and $\hat{\boldsymbol{\mu}}$ is the evolution of the location estimation. The depicted sphere is centered at the final estimated source and has radius $r_{min} = 0.5$ m. (b) Evolution of the estimated $\hat{\phi}$ (top), source estimation error (bottom).

converges in less than 120 s, with convergence occurring more rapidly as the number of robots increases, as expected from the numerical simulations. In all experiments, the robots' motions produce a decrease in the information metric. Videos of the experiments are shown in the supplementary material.

VI. Conclusions

In this paper, we proposed a novel multi-robot distributed active-sensing strategy to estimate the parameters of a source continuously releasing a substance in space. To enhance filter convergence, the robot motion optimizes an **A**-optimality information metric derived from the local Observability Gramian. The robots move in the direction that maximally improves this metric, while leveraging their current estimates to autonomously transition to more exploratory motions when necessary. A QP layer ensures safety constraints among robots while keeping the information bounded.

The proposed approach was validated through numerical simulations where it was compared against three baseline methods. The results demonstrated a higher success rate and more efficient motion trajectories, especially for smaller robot groups. Additionally, experiments with drones confirmed the framework's ability to generate collision-free and informative motions also in practice.

Further works could consider multiple moving sources, time-varying release rates, or battery-related energy con-

IEEE Robotics and Automation Letters (RA-L) paper, presented at ICRA 2026, Vienna, Austria. Cite as RA-L paper.

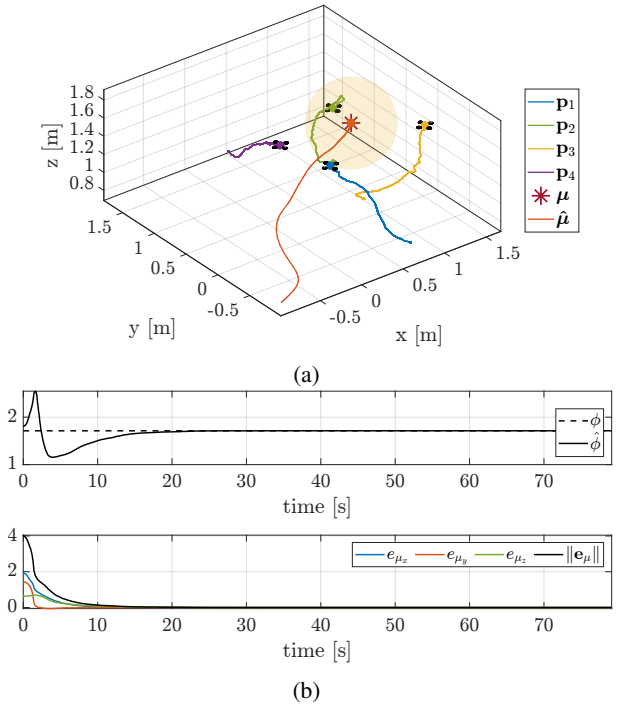

Fig. 7: $N = 4$, $\bar{u} = 0.2\ m/s$ (a) Drones' paths acquired from the motion capture system, the source location $\boldsymbol{\mu}$ is indicated with a star, and $\hat{\boldsymbol{\mu}}$ is the evolution of the location estimation. The depicted sphere is centered at the final estimated source and has radius r_{min}. (b) Evolution of the estimated $\hat{\phi}$ (top), source location estimation error (bottom).

straints, while experiments on a real field could provide further insight into the method's robustness. Future research could also address the problem of agent-source interactions, developing motion strategies that both optimize the information gain and minimize the robot-induced disturbances on the field.

REFERENCES

[1] T. Zhang, V. Qin, Y. Tang, and N. Li, "Distributed Information-Based Source Seeking," *IEEE Transactions on Robotics*, vol. 39, no. 6, pp. 4749–4767, Dec. 2023.

[2] G. Notomista, C. Pacchierotti, and P. R. Giordano, "Online Robot Trajectory Optimization for Persistent Environmental Monitoring," *IEEE Control Systems Letters*, vol. 6, pp. 1472–1477, 2022.

[3] G. Notomista, C. Pacchierotti, and P. R. Giordano, "Multi-robot persistent environmental monitoring based on constraint-driven execution of learned robot tasks," in *2022 International Conference on Robotics and Automation (ICRA)*. IEEE Press, 2022, p. 6853–6859.

[4] K. M. Lynch, I. B. Schwartz, P. Yang, and R. A. Freeman, "Decentralized Environmental Modeling by Mobile Sensor Networks," *IEEE Transactions on Robotics*, vol. 24, no. 3, pp. 710–724, Jun. 2008.

[5] M. Mantovani, F. Pratissoli, and L. Sabattini, "Distributed Coverage Control for Spatial Processes Estimation With Noisy Observations," *IEEE Robotics and Automation Letters*, vol. 9, no. 5, pp. 4431–4438, May 2024.

[6] D. Jang, J. Yoo, C. Y. Son, D. Kim, and H. J. Kim, "Multi-Robot Active Sensing and Environmental Model Learning With Distributed Gaussian Process," *IEEE Robotics and Automation Letters*, vol. 5, no. 4, pp. 5905–5912, Oct. 2020.

[7] M. L. Elwin, R. A. Freeman, and K. M. Lynch, "Distributed Environmental Monitoring With Finite Element Robots," *IEEE Transactions on Robotics*, vol. 36, no. 2, pp. 380–398, Apr. 2020.

[8] G. M. Hoffmann and C. J. Tomlin, "Mobile Sensor Network Control Using Mutual Information Methods and Particle Filters," *IEEE Transactions on Automatic Control*, vol. 55, no. 1, pp. 32–47, Jan. 2010.

[9] S. Li, R. Kong, and Y. Guo, "Cooperative Distributed Source Seeking by Multiple Robots: Algorithms and Experiments," *IEEE/ASME Transactions on Mechatronics*, vol. 19, no. 6, pp. 1810–1820, Dec. 2014.

[10] B. Bayat, N. Crasta, H. Li, and A. Ijspeert, "Optimal search strategies for pollutant source localization," in *2016 IEEE/RSJ International Conference on Intelligent Robots and Systems (IROS)*, Oct. 2016, pp. 1801–1807.

[11] P. Ogren, E. Fiorelli, and N. Leonard, "Cooperative control of mobile sensor networks:Adaptive gradient climbing in a distributed environment," *IEEE Transactions on Automatic Control*, vol. 49, no. 8, pp. 1292–1302, Aug. 2004.

[12] L. Briñón-Arranz, L. Schenato, and A. Seuret, "Distributed Source Seeking via a Circular Formation of Agents Under Communication Constraints," *IEEE Transactions on Control of Network Systems*, vol. 3, no. 2, pp. 104–115, Jun. 2016.

[13] L. Briñón-Arranz, A. Renzaglia, and L. Schenato, "Multirobot Symmetric Formations for Gradient and Hessian Estimation With Application to Source Seeking," *IEEE Transactions on Robotics*, vol. 35, no. 3, pp. 782–789, Jun. 2019.

[14] A. Renzaglia and L. Briñón-Arranz, "Search and Localization of a Weak Source with a Multi-robot Formation," *Journal of Intelligent & Robotic Systems*, vol. 97, no. 3, pp. 623–634, Mar. 2020.

[15] J. Bautista, A. Acuaviva, J. Hinojosa, W. Yao, J. Jiménez, and H. G. de Marina, "Fully distributed and resilient source seeking for robot swarms," *arXiv preprint arXiv:2410.15921*, 2024.

[16] B. Du, K. Qian, C. Claudel, and D. Sun, "Multiagent Online Source Seeking Using Bandit Algorithm," *IEEE Transactions on Automatic Control*, vol. 68, no. 5, pp. 3147–3154, May 2023.

[17] R. Khodayi-mehr, W. Aquino, and M. M. Zavlanos, "Model-Based Active Source Identification in Complex Environments," *IEEE Transactions on Robotics*, vol. 35, no. 3, pp. 633–652, Jun. 2019.

[18] V. Christopoulos and S. Roumeliotis, "Adaptive Sensing for Instantaneous Gas Release Parameter Estimation," in *Proceedings of the 2005 IEEE International Conference on Robotics and Automation*, Apr. 2005, pp. 4450–4456.

[19] J. You, Y. Zhang, M. Li, K. Su, F. Zhang, and W. Wu, "Cooperative parameter identification of advection-diffusion processes using a mobile sensor network," in *2017 American Control Conference (ACC)*, May 2017, pp. 3230–3236.

[20] F. Pukelsheim, *Optimal design of experiments*. SIAM, 2006.

[21] J. Crank, *The Mathematics of Diffusion*, ser. Oxford science publications. Clarendon Press, 1979.

[22] A. T. Kamal, J. A. Farrell, and A. K. Roy-Chowdhury, "Information Weighted Consensus Filters and Their Application in Distributed Camera Networks," *IEEE Transactions on Automatic Control*, vol. 58, no. 12, pp. 3112–3125, Dec. 2013.

[23] G. Battistelli, L. Chisci, G. Mugnai, A. Farina, and A. Graziano, "Consensus-Based Linear and Nonlinear Filtering," *IEEE Transactions on Automatic Control*, vol. 60, no. 5, pp. 1410–1415, May 2015.

[24] J. Slotine and W. Li, *Applied Nonlinear Control*, ser. Prentice-Hall International Editions. Prentice-Hall, 1991.

[25] B. D. Anderson and J. B. Moore, *Optimal filtering*. Courier Corporation, 2005.

[26] A. J. Krener and K. Ide, "Measures of unobservability," in *Proceedings of the 48h IEEE Conference on Decision and Control (CDC) held jointly with 2009 28th Chinese Control Conference*, 2009, pp. 6401–6406.

[27] G. Besançon, *Nonlinear Observers and Applications*, ser. Lecture Notes in Control and Information Sciences. Springer Berlin Heidelberg, 2007.

[28] P. Salaris, M. Cognetti, R. Spica, and P. R. Giordano, "Online optimal perception-aware trajectory generation," *IEEE Transactions on Robotics*, vol. 35, no. 6, pp. 1307–1322, 2019.

[29] L. Balandi, N. De Carli, and P. R. Giordano, "Persistent monitoring of multiple moving targets using high order control barrier functions," *IEEE Robotics and Automation Letters*, vol. 8, no. 8, pp. 5236–5243, 2023.

[30] N. D. Carli, P. Salaris, and P. R. Giordano, "Multi-robot active sensing for bearing formations," in *2023 International Symposium on Multi-Robot and Multi-Agent Systems (MRS)*, 2023, pp. 184–190.

[31] A. D. Ames, S. Coogan, M. Egerstedt, G. Notomista, K. Sreenath, and P. Tabuada, "Control barrier functions: Theory and applications," in *2019 18th European Control Conference (ECC)*, 2019, pp. 3420–3431.

[32] J. A. Preiss, W. Hönig, G. S. Sukhatme, and N. Ayanian, "Crazyswarm: A large nano-quadcopter swarm," in *IEEE International Conference on Robotics and Automation (ICRA)*. IEEE, 2017, pp. 3299–3304.